SEISMIC INTERFEROMETRY IN PARABOLIC RADON DOMAIN

HENG ZHU[1], DE-LI WANG[1] and GEORGIOS P. TSOFLIAS[2]

[1] *College of Geo-Exploration Science and Technology, Jilin University, Changchun 130026, P.R. China. zhuheng129@gmail.com; wangdeli@jlu.edu.cn*
[2] *Department of Geology, The University of Kansas, Lawrence, KS 66045, U.S.A. tsoflias@ku.edu*

(Received March 24, 2014; revised version accepted November 20, 2014)

ABSTRACT

Zhu, H., Wang, D.-L. and Tsoflias, G.P., 2015. Seismic interferometry in parabolic Radon domain. *Journal of Seismic Exploration*, 24: 37-50.

Seismic interferometry can redatum sources to the receiver locations in the subsurface, without knowing the information about the medium between sources and receivers. Theoretically, the receivers should be enclosed by the sources; however, in practice this condition is difficult to satisfy. In addition, some trace gathers may be lost. This will cause spurious events in the virtual shot gathers. Since parabolic Radon transform can be used to restore the data with missing trace gathers, seismic interferometry based on parabolic Radon transform can avoid the effect of these missing shots or traces, and suppress the spurious events. In addition, computation time can be saved with this method because parabolic Radon transform can usually reduce the data volume. We demonstrate this method with synthetic data and OBS data collected in the South China Sea.

KEY WORDS: seismic interferometry, parabolic Radon domain, suppression of spurious events, cross-correlation, time-space domain.

INTRODUCTION

Seismic interferometry can retrieve Green's function by crosscorrelating seismic responses collected at different receiver locations. The theory can be applied to passive source records as well as controlled source records. The strict relation between crosscorrelation and Green's function requires simplifying assumptions (Wapenaar, 2010a); (1) the medium is lossless; (2) the receivers are enclosed by the sources. The practical limitation of data acquisition (finite aperture, incomplete source distribution and finite source bandwidth) may cause artifacts. Therefore, seismic interferometry only obtains approximated Green's function and the virtual source gather may contain artifacts.

0963-0651/15/$5.00

Seismic interferometry has become very popular in recent years. Many passive applications have been proposed, such as earthquake coda interferometry (Snieder et al., 2002; Shapiro and Campillo, 2004), surface-wave tomography (Shapiro et al., 2005; Gerstoft et al., 2006), body-wave interferometry (Roux et al., 2005; Miyazawa et al., 2008), or reflection seismic interferometry (Draganov et al., 2007). Wapenaar et al. (2010a, 2010b) give a review of seismic interferometry theory and its recent advances. De Ridder and Dellinger (2011) demonstrated passive interferometric imaging of Scholte-wave velocities using a few hours of data. Using local earthquakes, Minato et al. (2012) imaged the oceanic crust surface using a 3D array of OBS.

Controlled-source seismic interferometry has been used in vertical seismic profiling (Bakulin and Calvert, 2006; Vasconcelos et al., 2008), inverse vertical seismic profiling (Yu and Schuster, 2006), and crosswell data (Minato et al., 2011). This method is also applied in OBS or ocean-bottom cable (OBC) data: Mehta et al. (2007) illustrate the improvement in virtual source method (Bakulin and Calvert, 2006) after wavefield separation using synthetic data; elastic interferometry theory was proposed by Gaiser and Vasconcelos (2010) and applied in OBC data in shallow water for retrieving P-waves and P-to-S waves using refraction interferometry. Haines (2011) applied interferometric processing to deep-water OBS data using a large OBS array to image the shallow subsurface. Carriere and Gerstoft (2013) used OBS interferometry for deep-water subsurface imaging. Bharadwaj et al. (2012) generated supervirtual traces in OBS to increase signal-to-noise ratio (S/N) and facilitate the traveltime picking of far-offset traces and head waves.

The classical interferometry is based on crosscorrelation of seismic traces recorded at different locations. In many situations, it can be advantageous to replace the crosscorrelation by deconvolution. One of the advantages is that deconvolution compensates for the properties of the source wavelet; another advantage is that it is unnecessary to assume the medium is lossless. Snieder et al. (2006) deconvolve passive responses observed at different depth levels and show that this leads to an estimate of the impulse response. Metha et al. (2007) use a similar approach to estimate the near-surface properties of the earth from passive recordings in a vertical borehole. Various authors have shown that multidimensional deconvolution applied to controlled-source data with receivers at a constant depth level can obtain the response of a redatumed source without needing a model of the subsurface. Wapenaar and Verschuur (1996) and Amundsen (1999) use multidimensional deconvolution (MDD) of wavefields recorded at the ocean bottom to obtain the response of the subsurface without ocean-bottom and surface-related multiples. Schuster and Zhou (2006) and Wapenaar et al. (2008b) discuss multidimensional deconvolution (MDD) of controlled-source data in the context of seismic interferometry. For the crosscorrelation based seismic interferometry, under the high-frequency approximation, this process can be viewed as cancellation of a raypath from a

physical source to two different receivers, and then summed over all sources (Schuster et al., 2004). The entire process is done in the time-space (t-x) domain or in its equivalent frequency domain. In this case, if a large number of traces need to be crosscorrelated, the process can be computationally intensive, especially in the time domain. In addition, the missing shots or traces will cause spurious events in virtual shot gathers.

Parabolic Radon transform cannot only be used to attenuate noise and multiples in seismic records, but also to restore the data with missing traces or shots (Kabir and Verschuur, 1995; Darche, 1990; Trad, 2002). So applying the seismic interferometry in the parabolic Radon domain can avoid the effect of missing traces or shots and suppress spurious events.

In this paper, we propose seismic interferometry based on parabolic Radon transform. The original time-space data is transformed into parabolic Radon domain and the virtual shot gathers are obtained by crosscorrelating the traces with the same curvature of the parabola and summing over all curvature traces. We illustrate the improvement of the resulting image by comparing with that obtained in the t-x domain. Then we apply this method to synthetic data with missing shots or traces and demonstrate that it can alleviate the effect caused by those missing shots or traces. Finally, we apply it to a real OBS data and obtain the virtual shot gather.

THEORY

Seismic interferometry is based on extracting Green's function that characterizes wave propagation between two receivers by cross correlating the wave fields recorded by these receivers. A general derivation of the Green's function retrieval process between two receivers is based on the reciprocity theorem (Wapenaar, 2004; Schuster, 2009). In this paper, we focus only on the crosscorrelation-type interferometry, which is based on the far-field approximation. In the frequency domain, the kinematic responses of seismic retrieval using the cross-correlation-type interferometry can be written as

$$d(x_B|x_A,\omega) + d^*(x_B|x_A,\omega) = \int d(x_B|x_A,\omega)d^*(x_B|x_A,\omega)dx_S \quad . \qquad (1)$$

Here, the coordinate left of the vertical line represents the receiver position, and the coordinate at the right is the source position. x_S is the source position at the surface. The asterisk * represents the complex conjugate.

According to eq. (1), the virtual shot gather can be obtained by cross correlating the responses recorded at different locations and stacking over source locations. In this paper, we apply seismic interferometry in the parabolic Radon

domain. For a horizontally layered medium or slightly dipping layered medium, one requirement of this method is that the receiver which acts as virtual source has the same horizontal position as that of one active source on the surface as shown in Fig. 1, or that the minimum horizontal offset is an integer multiple of the source interval as illustrated in real OBS data. We position the active source X_{S0} at the horizontal location of the virtual source X_A on the surface and we set it as the origin. We divide all sources into two panels as shown in Fig. 1. The sources at the left of X_{S0} are referred as panel I and the sources at the right are panel II. Eq. (1) shows that the virtual shot gather contains a causal part and an anti-causal part. The main contributions to the virtual shot gather come from sources around stationary phase points. In this paper, we only consider the causal part of the virtual shot gather. As shown in Fig. 1, stationary phase analysis shows that stationary phase contributions to the causal part of response from x_A to x_B are from panel I. Thus, for the common receiver gather, we set as the origin and use the responses in panel I to replace the response in panel II to obtain the symmetric common receiver gather $d(x_A|x_S,\omega)$ and $d(x_B|x_S,\omega)$. It should be note that the distance between x_A and x_B must be small, so $d(x_B|x_S,\omega)$ is approximately symmetric with respect to the origin. These common receiver gathers are also valid for the causal part of the response in eq. (1).

The Parabolic Radon transform can be used to attenuate noise and multiples in data; it can also be used to restore the data. This method can be implemented either in the time domain or in the frequency domain. It can be seen as the summation of amplitudes along parabolic lines of constant curvature in the time domain and a phase shift determined by curvature and survey position in the frequency domain. In the frequency domain, the forward and inverse parabolic Radon transform can be given by (Zhou and Greenhalgh, 1994):

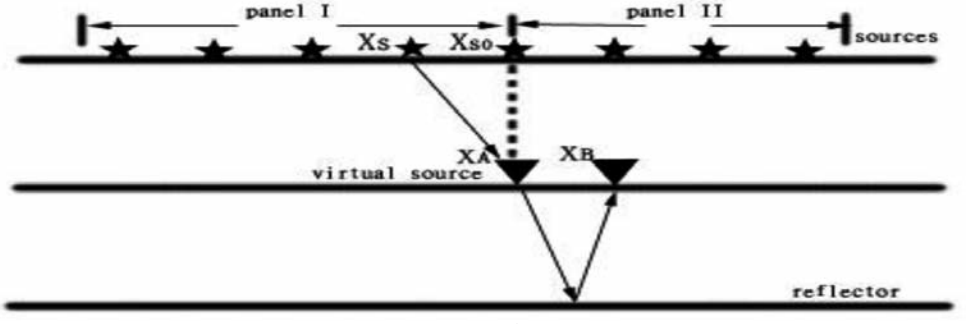

Fig. 1. Stationary phase point. The source X_{S0} is the origin with the same horizontal position as that of the virtual source x_A, the sources at its left are panel I. The sources at its right are panel II.

$$u(q,\omega) = \int d(x,\omega)\exp(i\omega q \cdot x^2)dx \quad , \tag{2}$$

$$d(x,\omega) = \int u(q,\omega)\exp(-i\omega q \cdot x^2)dq \quad , \tag{3}$$

Here, ω is the angle frequency, $d(x,\omega)$ is the recorded data, $u(q,\omega)$ is the transformed data, q represents the curvature of the parabola and x is the spatial variable denoting offset or receiver positions or source positions. In order to derive the interferometry relation in the parabolic Radon domain, we need to apply the parabolic Radon transform on common receiver gathers, so x represents source position in this paper.

According to eq. (2), transform $d(x_A|x_S,\omega)$ to the parabolic Radon domain

$$u_A(q,\omega) = \int d(x_A|x_S,\omega)\exp(i\omega q \cdot x_S^2)dx_S \quad , \tag{4}$$

Here, q is the curvature of the parabola, which depends on the position of receiver A. x_S is the source position.

According to eq. (2), the inverse Radon transform can be defined by

$$d(x_A|x_S,\omega) = \int u_A(q,\omega)\exp(-i\omega q \cdot x_S^2)dq \quad , \tag{5}$$

Then, the complex conjugate of in the frequency domain is given by:

$$d^*(x_A|x_S,\omega) = \int u_A^*(q,\omega)\exp(i\omega q \cdot x_S^2)dq \quad , \tag{6}$$

Inserting eq. (6) into eq. (3), we obtain

$$d(x_B|x_A,\omega) + d^*(x_B|x_A,\omega)$$

$$= \int\int d(x_B|x_S,\omega)u_A^*(q,\omega)\exp(i\omega q \cdot x_S^2)dqdx_S \quad , \tag{7}$$

Notice that $\int d(x_B|x_S,\omega)\exp(i\omega q \cdot x_S^2)dx_S$ in the above equation is the forward parabolic Radon transform. So eq. (7) can be rewritten as follows:

$$d(x_B|x_A,\omega) + d^*(x_B|x_A,\omega) = \int u_B(q,\omega)u_A^*(q,\omega)dq \quad . \tag{8}$$

Eq. (8) shows that in the parabolic Radon domain, the causal part of response can be obtained by cross correlating the traces that have the same value of curvature of the parabola and stacking over all q traces.

Suppose that the input seismic data are sorted as common shot gathers. The steps to perform seismic interferometry in the parabolic Radon domain can be described as follows:

1. For response from virtual source to its right receivers. Set source X_{S0} with the horizontal position of the virtual source as the origin, and then use the responses in panel I in Fig. 1 to replace the responses in panel II symmetrically to obtain the common receiver gather. For the response from virtual source to its left receivers, use the responses in panel II to obtain the common receiver gather.

2. Transform the common receiver gather in step 1 to the parabolic Radon domain.

3. Using eq. (8), perform crosscorrelation. Correlate q traces with the same value of curvature and sum over all q traces. Only the causal part of responses is used.

4. Loop step 3 over all the receivers.

In the next section, we test this method both on synthetic data and field data.

NUMERICAL EXAMPLE

Fig. 2 shows the P-wave velocity model we use for the synthetic test. This model has four layers. The first layer is a 100 m thick low velocity layer with V = 1500 m/s, the second layer has V = 2500 m/s, the third layer has V = 3500 m/s and the last layer has V = 4500 m/s. 250 receivers are located at depth z = 100 m with equal spacing of 10 m and the first receiver located at x = 0 m. 150 source locations are at the free surface (z = 0) and shot interval is 10 m. The first shot is excited at x = 500 m. After using seismic interferometry, the sources at the surface can be redatumed to the position of receivers at z = 100 m. So seismic interferometry can remove the propagation effect of overburden and get the source and receiver closer to the area of interest.

First, we perform seismic interferometry in the t-x domain by selecting a master trace at x = 1250 m as the virtual source and other traces as the receivers. After crosscorrelating the master trace with others and summing over all sources, the virtual shot gather is obtained as shown in Fig. 3b. For the parabolic Radon domain interferometry, we set the source at x = 1250 m (the same as the horizontal position of virtual source) on surface as the origin and obtain the symmetric common receiver gather with the method described above.

Using eq. (8), the virtual shot gather can be obtained by correlating the traces with the same curvature of the parabola and summing over all curvature traces. The result is shown in Fig. 3c. For comparison, the synthetic shot gather is shown in Fig. 3a.

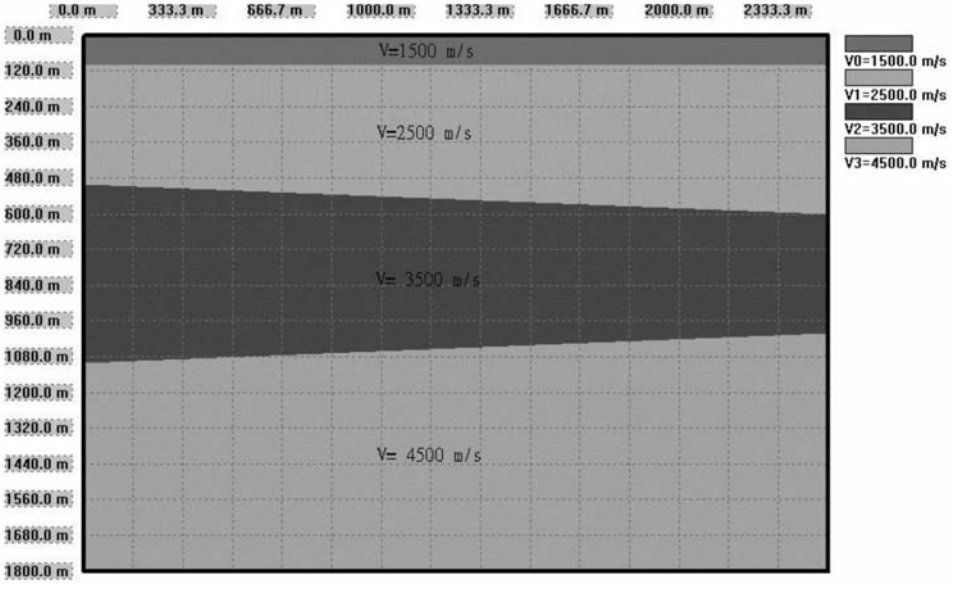

Fig. 2. Acoustical model used for the synthetic test. Model parameters are: (1) V = 1500 m/s, (2) V = 2500 m/s, (3) V = 3500 m/s, (4) V = 4500 m/s.

Through comparison, we can observe that the virtual shot gather using the t-x domain interferometry contains considerably more spurious events than the shot gather generated using the parabolic Radon domain interferometry. The far offset traces in Fig. 3b are not clear due to incomplete interferometry. For the virtual shot gather using the parabolic Radon domain interferometry (Fig. 3c), the reflections are correctly retrieved compared with the synthetic gather in Fig. 3a. Furthermore, far-offset responses are retrieved accurately and with greater clarity than using the t-x domain interferometry. Therefore, we can conclude that the parabolic Radon domain interferometry can reduce the effect caused by the limited source aperture. The reflection response indicated by black arrow in Fig. 3b is a non-physical event compared with the Fig. 3a. In Fig.3c, this event becomes very weak. So the parabolic Radon domain interferometry can suppress the spurious events.

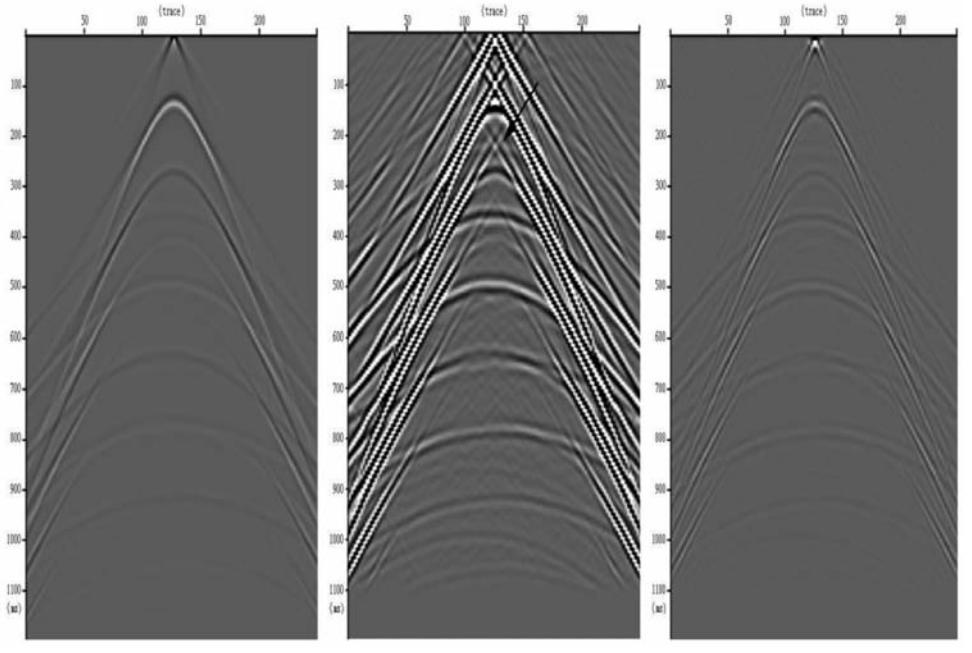

Fig. 3. Comparison of virtual shot gathers obtained by using time-space domain and parabolic Radon domain interferometry. (a) Synthetic gather generated by placing a source at x = 1250 m, z = 100 m and a line of receivers at z = 100 m. (b) The time-space domain interferometry. (c) The parabolic Radon domain interferometry.

SPARSE SOURCE DISTRIBUTION

In practice, seismic sources may be distributed irregularly or some traces could be missing. These will cause spurious events in reconstructing the virtual source gathers. The parabolic Radon transform can be used to interpolate the data with missing traces. Based on this property of the parabolic Radon transform, we do seismic interferometry in the parabolic Radon domain to suppress spurious events caused by missing data. In this section, we present two synthetic models testing this method.

In the first model the sources are reduced from 150 shots to 100 shots by removing the side sources as shown in Fig. 4a.

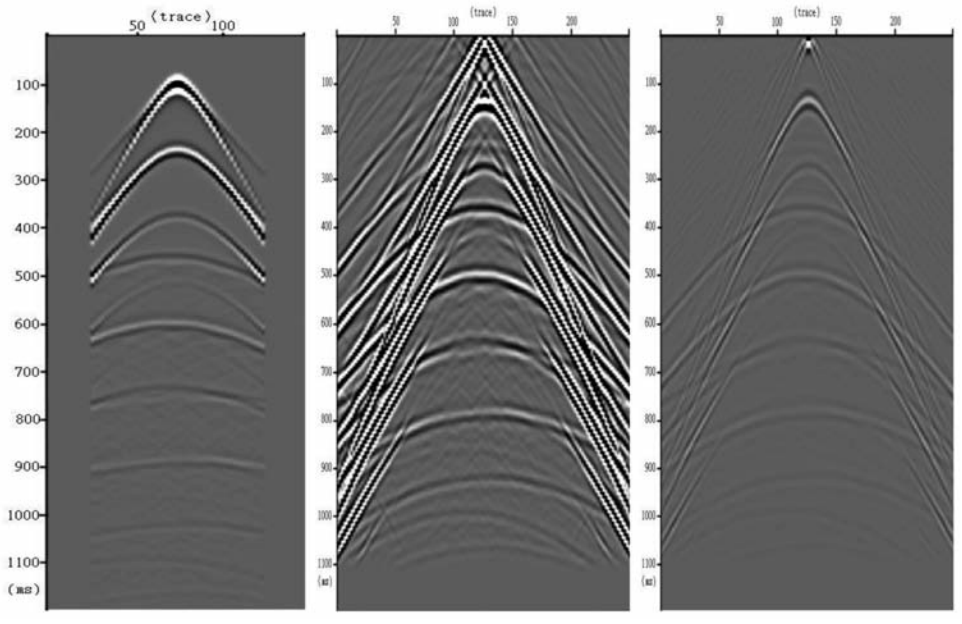

Fig. 4. Comparison of virtual shot gathers between the t-x domain interferometry and the parabolic Radon domain interferometry with 100 shots. (a) The original common receiver gather at x = 1250 m with 50 shots removed. (b) The time-space domain interferometry. (c) The parabolic Radon domain interferometry.

Through comparison, we observe that the missing shots cause additional noise when we perform seismic interferometry in the time-space domain (Fig. 4b). The virtual shot gather obtained by the parabolic Radon domain interferometry is still clear.

In another test, we reduce the total shots to 80, but this time, the middle part of the common receiver gathers (from 45 to 65) are removed as shown in Fig. 5a. Fig. 5b shows that once again a noisy result is obtained with the time-space domain interferometry. For the parabolic Radon domain interferometry, the response indicated by the box in Fig. 5c becomes a little noisy, but the reconstructed reflections are still clear. The missing shot gathers have little effect on the virtual source gather by using the parabolic Radon domain interferometry.

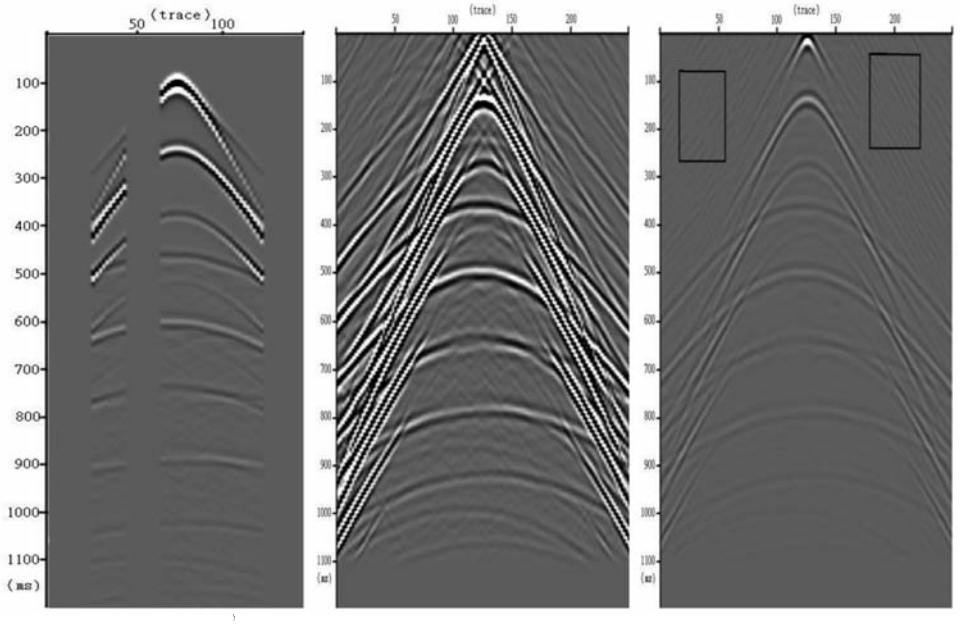

Fig. 5. Comparison of virtual shot gathers between the t-x domain interferometry and the parabolic Radon domain interferometry with 80 shots. (a) The original common receiver gather at 1250 m with 70 shots removed. (b) The time-space domain interferometry. (c) The parabolic Radon domain interferometry.

Numerical tests show that the parabolic Radon transform can be used to interpolate the incomplete data. This property can be used to suppress the spurious events in seismic interferometry. The results show that the parabolic Radon domain interferometry is less sensitive to the missing shots than the time-space domain interferometry.

FIELD EXAMPLE: REDATUMING THE OBS DATA

In this section, we apply the parabolic Radon domain interferometry to a real OBS data collected in the South China Sea. The geometry consists of 240 traces (spaced every 12.5 m) and 240 shots (spaced every 25 m) near the sea surface. The recording time is 2.4 s. The nearest offset is 350 m and the source moves with the line of receivers. This creates a problem for using seismic

interferometry. We need to first sort the common receiver gathers from the common shot gathers. This means that some parts of the data are not suitable for seismic interferometry. We sort 70 shot gathers (100 traces per shot) as shown in Fig. 6a. The shot interval and trace interval are both 25 m. The resulting shot gathers simulate a fixed receiver line with moving sources.

We choose receiver 100 as the virtual source. Fig. 6b shows the virtual shot gather using the t-x domain seismic interferometry. We can observe that it contains many spurious events and the resolution is low. The far offset responses are noisy and not clear. For the parabolic Radon domain seismic interferometry, we set the horizontal position of receiver 100 on surface as the origin. But at this position, there is no source. In this case, we assume the 14 sources between the nearest offset are missing which is similar with the cases

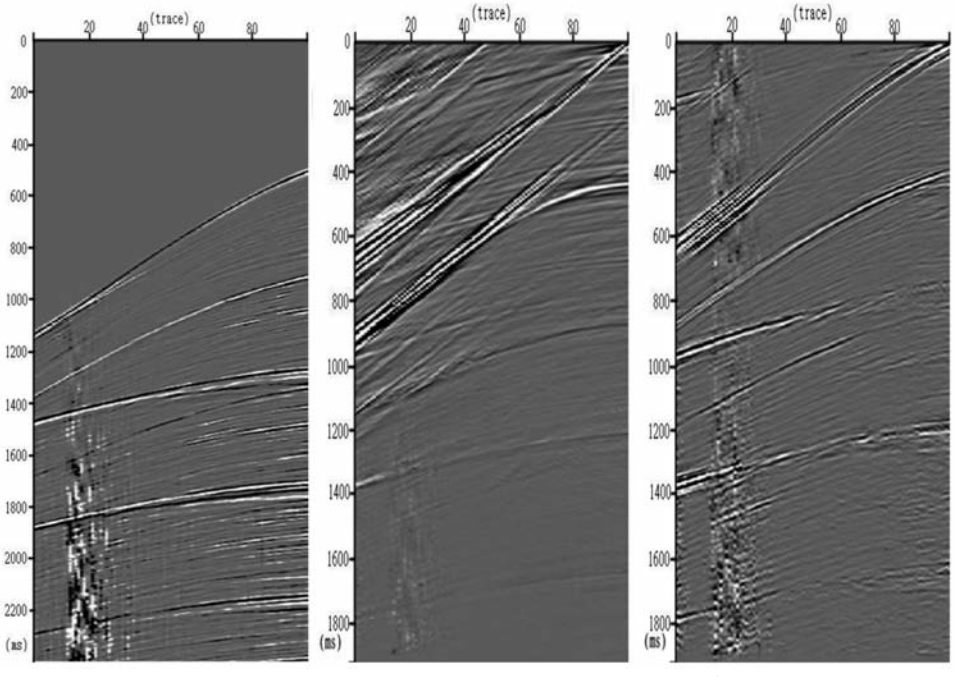

Fig. 6. Comparison of virtual shot gathers between the t-x domain interferometry and the parabolic Radon domain interferometry. (a) The original shot gather with 100 traces. (b) The virtual shot gather obtained by the time-space domain interferometry. (c) The virtual shot gather obtained by the parabolic Radon domain interferometry.

illustrated in the last section and obtain the symmetric common receiver gather with the method as described above. Fig. 6c shows the virtual shot gather obtained by using the parabolic Radon domain interferometry. It can be seen that Fig. 6c contains fewer spurious events and that the far offset responses are reconstructed clearly. The resolution of the profile is improved dramatically when employing parabolic Radon domain interferometry.

CONCLUSIONS

We propose seismic interferometry in the parabolic Radon domain. We demonstrate use of the method in controlled source data. The parabolic Radon transform can be used to restore incomplete data. The parabolic Radon domain seismic interferometry makes use of this property. Using seismic interferometry in the parabolic Radon domain can suppress spurious events associated with incomplete data. We employed synthetic tests to illustrate that this approach can suppress the spurious events and improve the resolution of the profile. Then we demonstrate that the parabolic Radon domain interferometry can avoid the effect of missing shots or traces. Finally we apply this method to real OBS data and demonstrate the effectiveness of this method.

ACKNOWLEDGEMENT

This paper is supported by the National Natural Science Foundation of China (Grant No. 41374108).

REFERENCES

Amundsen, L., 1999. Elimination of free surface-related multiples without need of the source wavelet. Expanded Abstr., 69th Ann. Internat. SEG Mtg., Houston: 1064-1067.

Bakulin, A. and Calvert, R., 2006. The virtual source method: Theory and case study. Geophysics, 71: SI139-SI150. doi: 10.1190/1.2216190.

Bharadwaj, P., Schuster, G.T., Mallinson, I. and Dai, W., 2012. Theory of supervirtual refraction interferometry. Geophys. J. Internat., 188: 263-273. doi: 10.1111/gji.2012.188.issue-1.

Carriere, O. and Gerstoft, P., 2013. Deep-water subsurface imaging using OBS interferometry. Geophysics, 78(2): Q15-Q24. doi: 10.1190/geo2012-0241.1.

De Ridder, S. and Dellinger, J., 2011. Ambient seismic noise eikonal tomography for near-surface imaging at Valhall. The Leading Edge, 30: 506-512. doi: 10.1190/1.3589108.

Darche, G., 1990. Spatial interpolation using a fast parabolic transform. Expanded Abstr., 60th Ann. Internat. SEG Mtg., San Francisco: 1647-1650.

Draganov, D., Wapenaar, C.P.A., Mulder, W., Singer, J. and Verdel, A., 2007. Retrieval of reflections from seismic background-noise measurements. Geophys. Res. Lett., 34: L04305. doi: 10.1029/2006GL028735.

Gaiser, J. and Vasconcelos, I., 2010. Elastic interferometry for ocean bottom cable data: Theory and examples. Geophys. Prosp., 58: 347-360. doi: 10.1111/(ISSN) 1365-2478.

Gerstoft, P., Sabra, K.G., Roux, P., Kuperman, W.A. and Fehler, M.C., 2006. Green's functions extraction and surface-wave tomography from microseisms in southern California. Geophysics, 71 (4): SI23-SI31. doi: 10 .1190/1.2210607.

Haines, S.S., 2011. PP and PS interferometric images of near-seafloor sediments. Expanded Abstr., 81st Ann. Internat. SEG Mtg., San Antonio: 1288-1292.

Kabir, M.M.N. and Verschuur, D.J., 1995. Restoration of missing offsets by parabolic Radon transform. Geophys. Prosp., 43: 347-368.

Miyazawa, M., Snieder, R. and Venkataraman, A., 2008. Application of seismic interferometry to extract P- and S-wave propagation and observation of shear-wave splitting from noise data at Cold Lake, Alberta, Canada. Geophysics, 73 (4): D35-D40. doi: 10.1190/1.2937172.

Mehta, K., Snieder, R. and Graizer, V., 2007. Extraction of near-surface properties for a lossy layered medium using the propagator matrix. Geophys. J. Internat., 169: 271-280.

Mehta, K., Bakulin, A., Sheiman, J., Calvert, R. and Snieder, R., 2007. Improving the virtual source method by wavefield separation. Geophysics, 72 (4): V79-V86. doi: 10.1190/1.2733020.

Minato, S., Matsuoka, T., Tsuji, T., Draganov, D., Hunziker, J. and Wapenaar, C.P.A., 2011. Seismic interferometry using multidimensional deconvolution and crosscorrelation for crosswell seismic reflection data without borehole sources. Geophysics, 76 (1): SA19-SA34, doi: 10.1190/1.3511357.

Minato, S., Tsuji, T., Matsuoka, T. and Obana, K., 2012. Crosscorrelation of earthquake data using stationary phase evaluation: Insight into reflection structures of oceanic crust surface in the Nankai Trough. Internat. J. Geophys., 25: 1-8. doi: 10.1155/2012/101545.

Roux, P., Sabra, K.G., Gerstoft, P., Kuperman, W.A. and Fehler, M.C., 2005. P-waves from cross-correlation of seismic noise. Geophys. Res. Lett., 32: L19303. doi: 10.1029/2005GL023803.

Schuster, G.T., Yu, J., Sheng, J. and Rickett, J., 2004. Interferometric/daylight seismic imaging. Geophys. J. Internat., 157: 838-852.

Schuster, G.T. and Zhou, M., 2006. A theoretical overview of model-based and correlation-based redatuming methods. Geophysics, 71 (4): SI103-SI110.

Schuster, G.T., 2009. Seismic Interferometry. Cambridge University Press, Cambridge.

Snieder, R., Grêt, A. Douma, H. and Scales, J., 2002. Coda wave interferometry for estimating nonlinear behavior in seismic velocity. Science, 295: 2253-2255. doi: 10.1126/science.1070015.

Snieder, R., Sheiman, J. and Calvert, R., 2006. Equivalence of the virtual- source method and wave-field deconvolution in seismic interferometry. Phys. Rev. E, 73: 066620.

Shapiro, N.M. and Campillo, M., 2004. Emergence of broadband Rayleigh waves from correlations of the ambient seismic noise. Geophys. Res. Lett., 31: L07614. doi: 10.1029/2004GL019491.

Shapiro, N.M., Campillo, M., Stehly, L. and Ritzwoller, M.H., 2005. High-resolution surface-wave tomography from ambient seismic noise. Science, 307: 1615-1618. doi: 10.1126/science.1108339.

Trad, D., Ulrych, T.J. and Sacchi, M.D., 2002. Accurate interpolation with high-resolution time-variant Radon transforms. Geophysics, 67(2): 644-656.

Vasconcelos, I., Snieder, R. and Hornby, B., 2008. Imaging internal multiples from subsalt VSP data - Examples of target-oriented interferometry. Geophysics, 73(4): S157-S168. doi: 10.1190/1.2944168.

Wapenaar, C.P.A. and Verschuur, D.J., 1996. Processing of ocean bottom data: The Dolphin Project. Delft University of Technology, 6.1-6.26.

Wapenaar, C.P.A., 2004. Retrieving the elastodynamic Green's function of an arbitrary inhomogeneous medium by cross correlation. Phys. Rev. Lett., 93: 254301. doi: 10.1103/PhysRevLett.93.254301.

Wapenaar, C.P.A., Slob, E. and Snieder, R., 2008b. Seismic and electromagnetic controlled-source interferometry in dissipative media. Geophys. Prosp., 56: 419-434.

Wapenaar, C.P.A., Draganov, D., Snieder, R., Campman, X. and Verdel, A. 2010a. Tutorial on seismic interferometry: part 1 - basic principles and applications. Geophysics, 75: A195-A209.

Wapenaar, C.P.A., Slob, E., Snieder, R. and Curtis, A., 2010b. Tutorial on seismic interferometry: Part 2 - Underlying theory and new advances. Geophysics, 75: A211-A227. doi: 10.1190/1.3463440.

Yu, J. and Schuster, G.T., 2006. Crosscorrelogram migration of inverse vertical seismic profile data. Geophysics, 71: S1-S11. doi: 10 .1190/1.2159056.

Zhou, B. and Greenhalgh, S.A., 1994. Linear and parabolic t-p transforms revisited. Geophysics, 59: 1133-1149.